
Direct transformation of crystalline MoO₃ into few-layers MoS₂

Felix Carrascoso ^{*1}, Gabriel Sanchez-Santolino ⁺¹, Chun-wei Hsu ^{1,2}, Norbert M. Nemes ³, Almudena Torres-Pardo ⁴, Patricia Gant ¹, Federico J. Mompeán ¹, Kouros Kalantar-zadeh ⁵, José A. Alonso ¹, Mar García-Hernández ¹, Riccardo Frisenda ¹, Andres Castellanos-Gomez ^{*1}

¹ Materials Science Factory. Instituto de Ciencia de Materiales de Madrid (ICMM-CSIC), Madrid, E-28049, Spain.

² Kavli Institute of Nanoscience. Delft University of Technology. Delft 2600 GA, The Netherlands.

³ Departamento de Física de Materiales, Universidad Complutense de Madrid, E-28040 Madrid, Spain.

⁴ Departamento de Química Inorgánica, Facultad de Químicas, Universidad Complutense, 28040- Madrid, Spain.

⁵ School of Chemical Engineering, University of New South Wales, Kensington, NSW 2052, Australia.

* Correspondence: felix.c@csic.es, andres.castellanos@csic.es

Abstract: We fabricate large-area atomically thin MoS₂ layers through the direct transformation of crystalline molybdenum trioxide (MoO₃) by sulfurization at relatively low temperatures. The obtained MoS₂ sheets are polycrystalline (~10-20 nm single-crystal domain size) with areas of up to 300×300 μm² with 2-4 layers in thickness and show a marked p-type behaviour. The synthesized films are characterized by a combination of complementary techniques: Raman spectroscopy, X-ray diffraction, transmission electron microscopy and electronic transport measurements.

1. Introduction

Two-dimensional (2D) transition metal dichalcogenides (TMDCs) have recently gained interest among the scientific community to solve the weakness of the lack of a bandgap in graphene, which limits its applications in field-effect transistors and digital integrated circuits [1]. The TMDC molybdenum disulphide (MoS₂) was the first 2D material with an intrinsic bandgap that was isolated [2] and it consists of S-Mo-S layers that are held by weak van der Waal forces in a trigonal prismatic structure [3–6]. In its bulk form, this material displays an indirect bandgap of about 1.2 eV; nevertheless, it becomes a direct bandgap semiconductor (1.8 eV) when it is thinned down to a monolayer [7]. In addition, when a single-layer MoS₂ is used as the channel in a field-effect transistor, it exhibits high in-plane mobility and large current ON/OFF ratio [8]. These are the reasons why molybdenum disulphide has attracted interest for electronic and optoelectronics applications [8–10]. Furthermore, it is an attractive candidate for energy conversion [11,12] and storage [13,14], hydrogen evolution reactions [15–17] or oxygen reduction reactions [18].

First methods that were reported for the synthesis of 2D MoS₂ consisted of mechanical and chemical exfoliation from bulk crystals [2,19,20] and, in fact, a lot of studies still use these methods since they provide high-quality single layers. However, these techniques present some problems like randomly deposited flakes, relatively small coverage area of material and a poor control over thickness. A solution for these issues is critical to achieve real-life electronic devices based on MoS₂

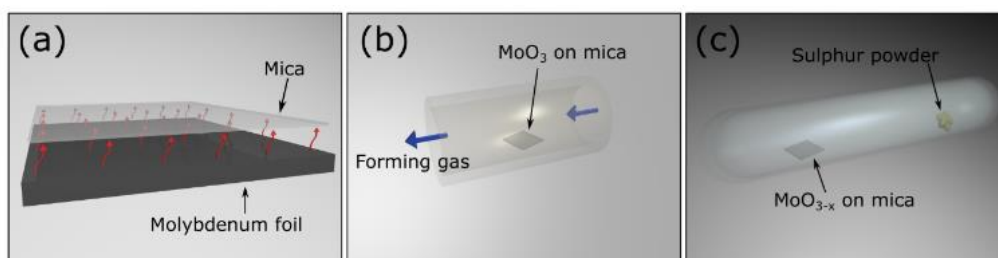


Figure 1. Cartoon of the process followed for the MoO₃ conversion into MoS₂. (a) MoO₃ sublimes from a hot molybdenum foil (540 °C) and it crystallizes onto a mica substrate. (b) MoO_{3-x} is formed after placing the MoO₃ in a tube furnace at 300 °C in a forming gas atmosphere for 24 hours. (c) Sulfuration process is performed in a closed glass ampoule at 500 °C - 600 °C.

and, therefore, synthesis of large-area MoS₂ films is a very active research area. The most explored methods to synthesise large-area MoS₂ thin films are the chemical vapour deposition (CVD) [21,22] and the sulfuration of sputtered molybdenum thin films [23–25].

Here, we explore an alternative route to obtain atomically thin MoS₂ layers: the direct transformation of crystalline molybdenum trioxide (MoO₃) layers into MoS₂ nanosheets by sulfurization at moderate temperatures. Up to now the sulfurization of crystalline MoO₃ have only demonstrated to produce MoS₂ fullerenes and nanotubes but here we demonstrate that it can be also employed to fabricate large area MoS₂ layers [26,27]. We characterized the resulting layers by Raman spectroscopy, X-ray diffraction and transmission electron microscopy, finding that the resulting layers show all the characteristics of polycrystalline MoS₂. We transferred the as-synthesized films to pre-patterned electrodes to fabricate electronic devices and we found that they are strongly p-doped, which can be an interesting feature to complement the marked n-doping of mechanically exfoliated or CVD grown MoS₂. Our synthesis method does not require a tube furnace with flow gas control as the sulfurization is carried out in a sealed ampoule, simplifying considerably its implementation, and reducing the cost.

2. Materials and Methods

The crystalline MoO₃ source is obtained by heating up a molybdenum foil (99.99% purity) to 540 °C in air using a laboratory hot plate. At this temperature, the MoO₃ starts to sublime. A mica substrate is placed above the hot molybdenum foil. The MoO₃ gas sublimed from the hot molybdenum foil crystallizes on the slightly cooler mica substrate placed on top, as we show in Figure 1(a). As reported by *Molina-Mendoza et al.* [26], this method produces continuous crystalline thin films through a van der Waals epitaxy process thanks to the van der Waals interaction with the mica surface. Note that in the van der Waals epitaxy process there is no need for lattice matching between the substrate and the grown MoO₃ overlayer.

Prior to the sulfuration of the MoO₃ crystals, they are reduced by heating them at 300 °C for 24 hours in a tube furnace in forming gas atmosphere, Figure 1(b). This process yields MoO_{3-x} crystals. We found that this step is crucial to avoid the evaporation of MoO₃ during the sulfuration process as MoO₃ is a highly volatile material. On the contrary, MoO₂ is a more stable oxide [28], in fact, by partially reducing the molybdenum trioxide we observe an improved stability of the material upon temperature increase. Then the MoO_{3-x} layers are converted to MoS₂ by a sulfuration process in a closed glass ampoule. The sample containing the MoO_{3-x} layers is sealed with sulphur powder at 10⁻⁵ mbar pressure. The ampoule is placed in a furnace at 500 °C for 5 hours and then the temperature is increased at 600 °C for another 5 hours. Once the sulfuration process is concluded, the temperature is slowly lowered to room temperature, Fig 1(c). The number of MoS₂ layers that we obtain depends

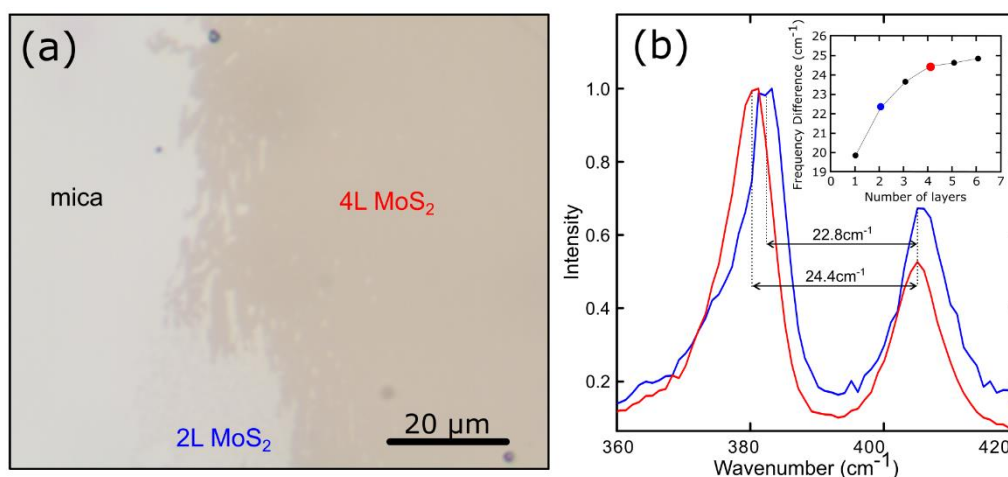


Figure 2. (a) Optical image of a large area MoS₂ on a mica substrate. (b) Raman Spectra of MoS₂ in different regions of the same sample. The inset displays the relation between the frequency difference of the two peaks and the number of layers of MoS₂.

on the starting MoO₃ thickness. Therefore, with this method we are able to obtain MoS₂ continuous layers covering most of the mica substrate with regions of up to 300×300 μm² with <5 layers in thickness, an example is shown in Figure 2(a). As discussed below, also single layer MoS₂ could be observed (see the discussion related to the scanning transmission electron microscopy results). It is important to note that, when we tried to sulfurize the as-grown MoO₃ layers, without the reduction step, we obtained thick MoS₂ crystallites randomly deposited on both the ampoule surface and on the substrate. Scanning transmission electron microscopy (STEM) data was acquired in an aberration-corrected JEOL JEM-ARM200cF electron microscope operated at 80 kV.

3. Results and discussion

3.1. Raman characterization

In Figure 2(a) we show an optical image of a thin and large-area MoS₂ film on mica. We employ Raman spectroscopy to characterize the MoS₂ film as this technique has been demonstrated to be a very powerful tool to characterize 2D materials [29,30]. Figure 2(b) presents the Raman spectra acquired on two locations (indicated in the figure) of the MoS₂ film shown in Figure 2(a). The characteristic E_{2g}¹ and A_{1g} phonon modes of MoS₂ (around 380 cm⁻¹ and 415 cm⁻¹) are clearly visible in the spectra [23,31]. One can determine the number of layers from the frequency difference between these two Raman modes. In the inset in Figure 2(b) we show the relation between this frequency difference and the number of layers of MoS₂, obtained from the literature [32,33], and we compare these values with those obtained in two spots in our sample to determine the number of layers finding that the MoS₂ specimen is composed of a bilayer and a four-layer region. We address the reader to the Supporting Information for a Raman map of another thin MoS₂ region.

3.2. XRD characterization

The crystal structure of the films has been characterized with X-ray diffraction (XRD). XRD was performed at room temperature on the initial sample (MoO₃ grown on mica 18 mm × 2 mm substrate) and on the final sample (MoS₂ obtained after the sulfuration process). Figure 3 illustrates the X-ray diffractograms that were taken for the initial sample and for the final sample in green and blue, respectively. In red, we also show the X-ray diffractogram for a bare mica substrate in order to be

able to differentiate the peaks that belong to the substrate from the peaks that correspond to the growth film.

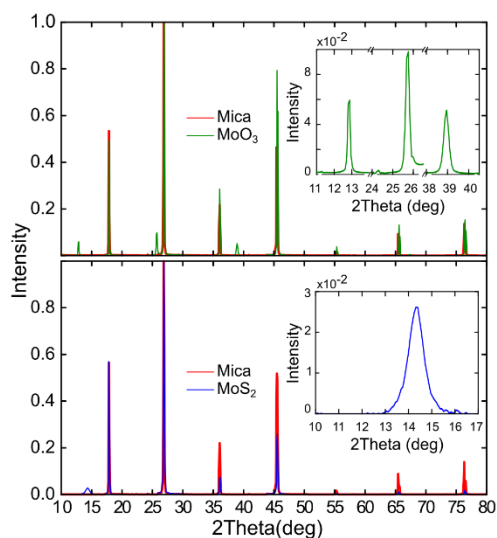


Figure 3. Comparison of XRD spectra of the sample shown in Fig. 2, at different steps: MoO₃ (initial) and MoS₂ (after sulfuration) in green and blue, respectively. XRD spectra of a mica substrate in red to distinguish it from the peaks of the layer analysed (insets).

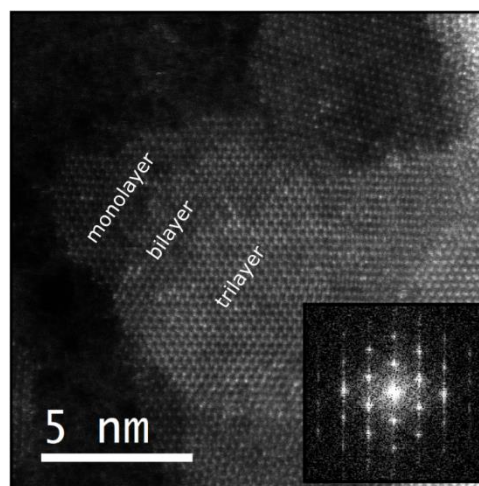


Figure 4. High magnification HAADF images of a MoS₂ thin film transferred over a holey Si₃N₄ membrane support. Inset shows FFT where a clearly hexagonal symmetry is exhibited.

Notice that the green spectrum exhibits peaks that correspond to (0 2 0), (0 4 0) and (0 6 0) reflections, which belong to the diffraction peaks of MoO₃. The appearance of the (0 *k* 0) peaks, parallel to the plane (0 1 0), is a product of a preferred orientation of the MoO₃ crystal with respect to the mica (0 0 1) surface due to the van der Waals epitaxy type of growth [34]. The blue spectrum obtained for the same sample after the sulfuration process shows a peak that corresponds to the (0 0 2) reflection of MoS₂ [6]. Thus, we further confirm that we are able to obtain MoS₂ from MoO₃ deposited onto a mica substrate. In some works it is proposed that the average thickness of a thin sample can be obtained from the analysis of the XRD peaks using the Scherrer equation ($D = k\lambda / \beta \cos\theta$, where k is the shape factor, λ is the X-ray wavelength, β is the full width at half maximum of the peak and 2θ is the scattering angle) [35,36]. By analysing the (002) peak of the MoS₂ XRD pattern we estimated a c-stacking height for the analyzed sample of 10 nm, which corresponds to 15 layers of MoS₂. Note that this value corresponds to the average thickness of the whole sample; however thinner regions (as those shown in Figure 2) can be found on it. It is also worth mentioning that the single-crystal domain size observed in our samples is also of the order of ~10 nm (see STEM discussion below) and thus it is not completely clear if the Scherrer equation provides accurate values of the average thickness of the sample or simply the single-crystal domain size.

3.2. STEM characterization

The crystal structure of the films can be further characterized in real space by STEM. Figure 4 displays a high-angle annular dark field (HAADF) image of a MoS₂ layer transferred over a holey Si₃N₄ membrane support by an all-dry deterministic transfer process [37]. In order to transfer the MoS₂ films on mica we stick a polydimethylsiloxane (PDMS) sheet on its surface and we immerse it in distilled water. Due to the hydrophilic character of mica, the water wedges between the MoS₂ and the mica surface separating the MoS₂ layer, which keeps attached to the PDMS substrate, from the

mica surface. The MoS₂ is easily transferred to the membrane by gently pressing the PDMS containing the MoS₂ film against the acceptor substrate and peeling it off slowly.

The STEM characterization indicates that the MoS₂ film is polycrystalline with a single-crystal domain size of 10-20 nm. Thinner regions can be found at the edges of the sulfurized film, where one can find monolayer, bilayer and trilayer areas (Figure 4 shows the edge of a MoS₂ film where mono-, bi- and tri-layer areas can be resolved). The fast Fourier transform (FFT) obtained from the monolayer region shows clearly the hexagonal symmetry of MoS₂.

3.2. Electrical characterization

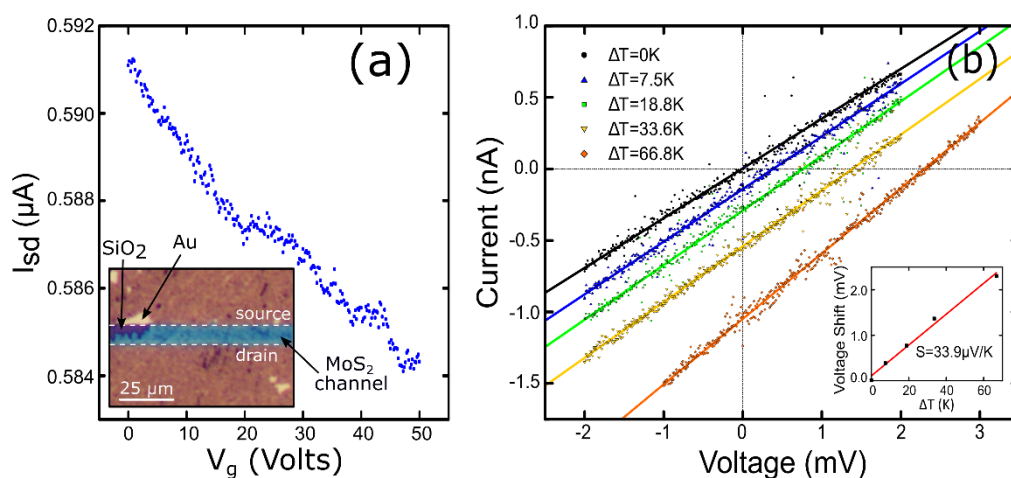


Figure 5. (a) Source-drain current *vs.* gate voltage measured in dark conditions and at $V_{sd} = 1$ V. The inset shows an optical image of the device measured (channel length = 10 μm , channel width = 1 mm). (b) Seebeck effect measurement on a MoS₂ layer on a mica substrate by applying a temperature difference between electrodes. The inset shows the linear relationship between the thermovoltage shift and the difference in temperature. The Seebeck coefficient can be readily extracted from the slope.

The electrical properties of the fabricated MoS₂ films have been characterized fabricating a field-effect device, by transferring a MoS₂ film onto a SiO₂/Si with pre-patterned drain-source electrodes separated 10 μm . Figure 5(a) shows the measured source-drain current *vs.* gate voltage (I_{sd} - V_g) characteristic for a fixed source-drain voltage of $V_{sd} = 1$ V. Surprisingly, we obtain a decrease in the source-drain current upon gate voltage increases without reaching the OFF state, which corresponds to a strong p-doped field effect behaviour. To confirm this fact, we performed a thermopower measurement. Figure 5(b) displays the *IV* characteristics acquired applying a temperature difference between the two electrodes. It can be seen how a positive voltage offset at zero current appears (thermoelectric voltage) when the temperature different increases. The inset shows the thermoelectric voltage versus the temperature difference. The Seebeck coefficient can be extracted from the slope of a linear fit to the data: $S = +33.9 \mu\text{V/K}$. This positive value confirms the p-doped nature of the MoS₂ film obtained by the direct sulfurization of crystalline MoO₃. The low magnitude of the Seebeck coefficient also indicates a high doping level. We have carried out preliminary Hall effect measurements backing up the p-type electrical behavior of the MoS₂ films observed in the Seebeck and electric-field measurements. Unfortunately, the large resistance of our samples precludes us from quantifying the charge carrier concentration as the electronics of our Hall effect measuring system is optimized for low impedance samples. The highly linear shape of the *IVs*, together with the high doping inferred from the shallow transconductance and low Seebeck coefficient, points to an Ohmic contact in the Au-MoS₂ junction. We have also estimated the resistivity of the device $\sim 100 \Omega\text{-cm}$,

which is significantly higher to that of single-crystal MoS₂ (~1-5 Ω·cm), [38,39] as expected from the small single-crystal domain size of our synthetic MoS₂ layers.

In order to get a deeper insight into the microscopic origin of this p-doping in our MoS₂ layers we have done an electron energy loss spectra (EELS) analysis of the STEM data (see Supporting Information). Apart from the presence of Mo and S, we found C (which could come from e-beam induced deposition of amorphous carbon during the STEM measurement), O and B. The presence of O could be due to an incomplete MoO₃ to MoS₂ transformation and the presence of B impurities could come from unintentional cross-contamination from the surface of the glass ampoules used during the growth. The presence of these foreign species could be a plausible source of the unexpected p-type doping.

Figure 6(a) represents the measured I_{sd} - V_{sd} characteristics in dark condition and under light excitation with different wavelengths. The gate voltage was set to $V_g = 0$ V during the measurement. Fiber coupled LED light sources were employed to illuminate the device. The inset of this figure zooms on the high voltage region of the traces to distinguish the differences induced upon illumination. The photocurrent as a function of the wavelength can be calculated from these data, as we show in Figure 6(b). This spectrum reveals that the maximum photocurrent value is located between 530 nm and 595 nm, whereas it decreases at longer wavelengths. We were not able of measuring a sizeable photocurrent beyond 740 nm as expected for multilayer MoS₂.

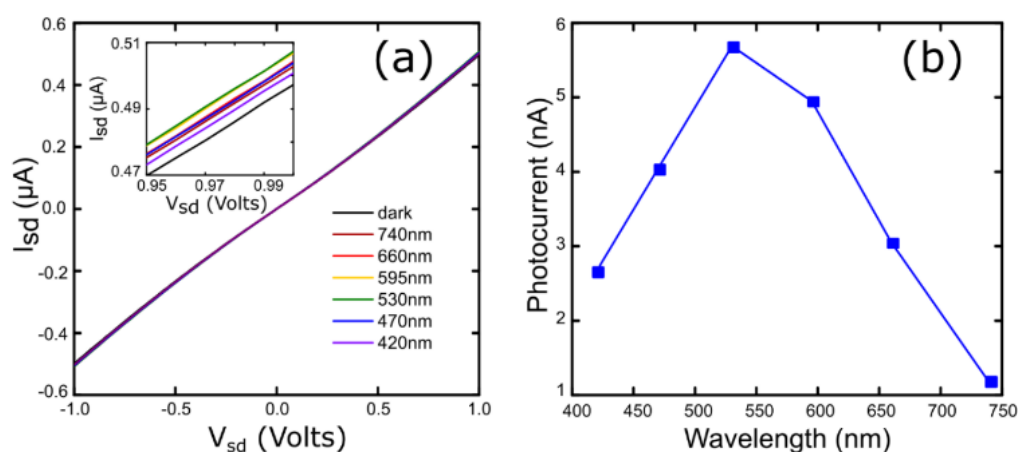


Figure 6. (a) I_{sd} - V_{sd} curves for different illumination wavelengths and $V_g = 0$ V. Inset shows a smaller range to facilitate the visualization of the generated photocurrent. (b) Photocurrent spectrum obtained from I_{sd} - V_{sd} curves.

4. Conclusions

In summary, we presented an alternative method to obtain atomically thin MoS₂ layers through the direct transformation of crystalline molybdenum trioxide (MoO₃) layers into MoS₂ nanosheets by sulfurization. The process can be carried out at moderate temperatures and using simple instrumentation. We obtained large area polycrystalline MoS₂ sheets 2 to 4 layers thick and we characterized them by Raman spectroscopy, X-ray diffraction and transmission electron microscopy. Regarding their electronic properties, they are strongly p-doped.

Funding: ACG acknowledge funding from the European Research Council (ERC) under the European Union's Horizon 2020 research and innovation programme (grant agreement n° 755655, ERC-StG 2017 project 2D-

TOPSENSE) and from the EU Graphene Flagship funding (Grant Graphene Core 2, 785219). JAA thanks the Spanish Ministry of Economy, Industry and Competitiveness (MINECO) for funding the project MAT2017-84496-R. RF acknowledges support from MINECO through a "Juan de la Cierva: formación" fellowship (2017 FJCI-2017-32919). GSS acknowledges financial support from MINECO (Juan de la Cierva 2015 program, FJCI-2015-25427).

Acknowledgments: We thank Carmen Munuera (ICMM-CSIC) and the National Center for Electron Microscopy (CNME; UCM, Madrid) for facilities.

Author Contributions: Conceptualization, Andres Castellanos-Gomez; Formal analysis, Felix Carrascoso, Gabriel Sanchez-Santolino, Chun-wei Hsu, Almudena Torres-Pardo, Federico Mompean and Riccardo Frisenda; Funding acquisition, Andres Castellanos-Gomez; Investigation, Felix Carrascoso, Gabriel Sanchez-Santolino, Chun-wei Hsu, Norbert M. Nemes, Almudena Torres-Pardo, Patricia Gant, Federico Mompean, Riccardo Frisenda and Andres Castellanos-Gomez; Project administration, Andres Castellanos-Gomez; Resources, Jose A. Alonso, Mar Garcian-Hernandez and Andres Castellanos-Gomez; Supervision, Norbert M. Nemes, Jose A. Alonso, Mar Garcian-Hernandez, Riccardo Frisenda and Andres Castellanos-Gomez; Writing – original draft, Felix Carrascoso and Andres Castellanos-Gomez; Writing – review & editing, Kourosh Kalantar-zadeh and Riccardo Frisenda.

References

- [1] Schwierz F 2010 Graphene transistors *Nat. Nanotechnol.* **5** 487–96
- [2] Novoselov K S, Jiang D, Schedin F, Booth T J, Khotkevich V V, Morozov S V and Geim A K 2005 Two-dimensional atomic crystals. *Proc. Natl. Acad. Sci. U. S. A.* **102** 10451–3
- [3] Verble J L and Wieting T J 1970 Lattice Mode Degeneracy in MoS_2 and Other Layer Compounds *Phys. Rev. Lett.* **25** 362–5
- [4] Mattheiss L F 1973 Band Structures of Transition-Metal-Dichalcogenide Layer Compounds *Phys. Rev. B* **8** 3719–40
- [5] Coehoorn R, Haas C, Dijkstra J, Flipse C J F, de Groot R A and Wold A 1987 Electronic structure of MoSe_2 , MoS_2 , and WSe_2 . I. Band-structure calculations and photoelectron spectroscopy *Phys. Rev. B* **35** 6195–202
- [6] Joensen P, Frindt R F and Morrison S R 1986 Single-layer MoS_2 *Mater. Res. Bull.* **21** 457–61
- [7] Mak K F, Lee C, Hone J, Shan J and Heinz T F 2010 Atomically Thin MoS_2 : A New Direct-Gap Semiconductor *Phys. Rev. Lett.* **105** 136805
- [8] Radisavljevic B, Radenovic A, Brivio J, Giacometti V and Kis A 2011 Single-layer MoS_2 transistors *Nat. Nanotechnol.* **6** 147–50
- [9] Radisavljevic B, Whitwick M B and Kis A 2011 Integrated Circuits and Logic Operations Based on Single-Layer MoS_2 *ACS Nano* **5** 9934–8
- [10] Yin Z, Li H, Li H, Jiang L, Shi Y, Sun Y, Lu G, Zhang Q, Chen X and Zhang H 2012 Single-Layer MoS_2 Phototransistors *ACS Nano* **6** 74–80
- [11] Fortin E and Sears W M 1982 Photovoltaic effect and optical absorption in MoS_2 *J. Phys. Chem. Solids* **43** 881–4
- [12] Wi S, Kim H, Chen M, Nam H, Guo L J, Meyhofer E and Liang X 2014 Enhancement of Photovoltaic Response in Multilayer MoS_2 Induced by Plasma Doping *ACS Nano* **8** 5270–81
- [13] Feng C, Ma J, Li H, Zeng R, Guo Z and Liu H 2009 Synthesis of molybdenum disulfide (MoS_2) for

- lithium ion battery applications *Mater. Res. Bull.* **44** 1811–5
- [14] Ding S, Zhang D, Chen J S and Lou X W (David) 2012 Facile synthesis of hierarchical MoS₂ microspheres composed of few-layered nanosheets and their lithium storage properties *Nanoscale* **4** 95–8
- [15] Li Y, Wang H, Xie L, Liang Y, Hong G and Dai H 2011 MoS₂ Nanoparticles Grown on Graphene: An Advanced Catalyst for the Hydrogen Evolution Reaction *J. Am. Chem. Soc.* **133** 7296–9
- [16] Huang X, Zeng Z, Bao S, Wang M, Qi X, Fan Z and Zhang H 2013 Solution-phase epitaxial growth of noble metal nanostructures on dispersible single-layer molybdenum disulfide nanosheets *Nat. Commun.* **4** 1444
- [17] Ye G, Gong Y, Lin J, Li B, He Y, Pantelides S T, Zhou W, Vajtai R and Ajayan P M 2016 Defects Engineered Monolayer MoS₂ for Improved Hydrogen Evolution Reaction *Nano Lett.* **16** 1097–103
- [18] Wang T, Gao D, Zhuo J, Zhu Z, Papakonstantinou P, Li Y and Li M 2013 Size-Dependent Enhancement of Electrocatalytic Oxygen-Reduction and Hydrogen-Evolution Performance of MoS₂ Particles *Chem. - A Eur. J.* **19** 11939–48
- [19] Coleman J N, Lotya M, O'Neill A, Bergin S D, King P J, Khan U, Young K, Gaucher A, De S, Smith R J, Shvets I V., Arora S K, Stanton G, Kim H-Y, Lee K, Kim G T, Duesberg G S, Hallam T, Boland J J, Wang J J, Donegan J F, Grunlan J C, Moriarty G, Shmeliov A, Nicholls R J, Perkins J M, Grievson E M, Theuwissen K, McComb D W, Nellist P D and Nicolosi V 2011 Two-Dimensional Nanosheets Produced by Liquid Exfoliation of Layered Materials *Science* **331** 568–71
- [20] Li H, Wu J, Yin Z and Zhang H 2014 Preparation and Applications of Mechanically Exfoliated Single-Layer and Multilayer MoS₂ and WSe₂ Nanosheets *Acc. Chem. Res.* **47** 1067–75
- [21] Lee Y-H, Zhang X-Q, Zhang W, Chang M-T, Lin C-T, Chang K-D, Yu Y-C, Wang J T-W, Chang C-S, Li L-J and Lin T-W 2012 Synthesis of Large-Area MoS₂ Atomic Layers with Chemical Vapor Deposition *Adv. Mater.* **24** 2320–5
- [22] Lee Y-H, Yu L, Wang H, Fang W, Ling X, Shi Y, Lin C-T, Huang J-K, Chang M-T, Chang C-S, Dresselhaus M, Palacios T, Li L-J and Kong J 2013 Synthesis and Transfer of Single-Layer Transition Metal Disulfides on Diverse Surfaces *Nano Lett.* **13** 1852–7
- [23] Kong D, Wang H, Cha J J, Pasta M, Koski K J, Yao J and Cui Y 2013 Synthesis of MoS₂ and MoSe₂ Films with Vertically Aligned Layers *Nano Lett.* **13** 1341–7
- [24] Zhan Y, Liu Z, Najmaei S, Ajayan P M and Lou J 2012 Large-Area Vapor-Phase Growth and Characterization of MoS₂ Atomic Layers on a SiO₂ Substrate *Small* **8** 966–71
- [25] Lee K, Gatensby R, McEvoy N, Hallam T and Duesberg G S 2013 High-Performance Sensors Based on Molybdenum Disulfide Thin Films *Adv. Mater.* **25** 6699–702
- [26] Molina-Mendoza A J, Lado J L, Island J O, Niño M A, Aballe L, Foerster M, Bruno F Y, López-Moreno A, Vaquero-Garzon L, van der Zant H S J, Rubio-Bollinger G, Agraït N, Pérez E M, Fernández-Rossier J and Castellanos-Gomez A 2016 Centimeter-Scale Synthesis of Ultrathin Layered MoO₃ by van der Waals Epitaxy *Chem. Mater.* **28** 4042–51
- [27] Burns R P, DeMaria G, Drowart J and Grimley R T 1960 Mass Spectrometric Investigation of the Sublimation of Molybdenum Dioxide *J. Chem. Phys.* **32** 1363–6
- [28] Li X L and Li Y D 2003 Formation of MoS₂ inorganic fullerenes (IFs) by the reaction of MoO₃ nanobelts and S *Chem. Eur. J.* **9** 2726–31
- [29] Castellanos-Gomez A, Querada J, van der Meulen H P, Agraït N and Rubio-Bollinger G 2016 Spatially

- resolved optical absorption spectroscopy of single- and few-layer MoS₂ by hyperspectral imaging *Nanotechnology* **27** 115705
- [30] Splendiani A, Sun L, Zhang Y, Li T, Kim J, Chim C-Y, Galli G and Wang F 2010 Emerging Photoluminescence in Monolayer MoS₂ *Nano Lett.* **10** 1271–5
- [31] Lee C, Yan H, Brus L E, Heinz T F, Hone J and Ryu S 2010 Anomalous Lattice Vibrations of Single- and Few-Layer MoS₂ *ACS Nano* **4** 2695–700
- [32] Iguiñiz N, Frisenda R, Bratschitsch R, Castellanos-Gomez A and Castellanos-Gomez A 2019 Revisiting the Buckling Metrology Method to Determine the Young's Modulus of 2D Materials *Adv. Mater.* **31** 1807150
- [33] Castellanos-Gomez A, Barkelid M, Goossens A M, Calado V E, Van Der Zant H S J and Steele G A 2012 Laser-thinning of MoS₂: On demand generation of a single-layer semiconductor *Nano Lett.* **12** 3187–92
- [34] Geng D Y, Zhang Z D, Zhang M, Li D, Song X P and Hu K Y 2004 Structure and surface characterization of α -MoO₃ whiskers synthesized by an oxidation process *Scr. Mater.* **50** 983–6
- [35] Chang K, Li M, Wang T, Ouyang S, Li P, Liu L and Ye J 2015 Drastic Layer-Number-Dependent Activity Enhancement in Photocatalytic H₂ Evolution over n MoS₂/CdS ($n \geq 1$) Under Visible Light *Adv. Energy Mater.* **5** 1402279
- [36] Iqbal S, Pan Z and Zhou K 2017 Enhanced photocatalytic hydrogen evolution from: In situ formation of few-layered MoS₂/CdS nanosheet-based van der Waals heterostructures *Nanoscale* **9** 6638–42
- [37] Castellanos-Gomez A, Buscema M, Molenaar R, Singh V, Janssen L, van der Zant H S J H S J and Steele G A G A 2014 Deterministic transfer of two-dimensional materials by all-dry viscoelastic stamping *2D Mater.* **1** 011002
- [38] Giannazzo F, Fisichella G, Piazza A, Agnello S and Roccaforte F 2015 Nanoscale inhomogeneity of the Schottky barrier and resistivity in MoS₂ multilayers *Phys. Rev. B* **92** 81307
- [39] Eda G, Yamaguchi H, Voiry D, Fujita T, Chen M and Chhowalla M 2011 Photoluminescence from chemically exfoliated MoS₂. *Nano Lett.* **11** 5111–6

Supporting Information: Direct transformation of crystalline MoO₃ into few-layers MoS₂

Felix Carrascoso *¹, Gabriel Sanchez-Santolino †¹, Chun-wei Hsu ^{1,2}, Norbert M. Nemes ³, Almudena Torres-Pardo ⁴, Patricia Gant ¹, Federico J. Mompeán ¹, Kourosh Kalantar-zadeh ⁵, José A. Alonso ¹, Mar García-Hernández ¹, Riccardo Frisenda ¹, Andres Castellanos-Gomez *¹

1 Materials Science Factory. Instituto de Ciencia de Materiales de Madrid (ICMM-CSIC), Madrid, E-28049, Spain.

2 Kavli Institute of Nanoscience. Delft University of Technology. Delft 2600 GA, The Netherlands.

3 Departamento de Física de Materiales, Universidad Complutense de Madrid, E-28040 Madrid, Spain.

4 Departamento de Química Inorgánica, Facultad de Químicas, Universidad Complutense, 28040- Madrid, Spain.

5 School of Chemical Engineering, University of New South Wales, Kensington, NSW 2052, Australia.

* Correspondence: felix.c@csic.es, andres.castellanos@csic.es

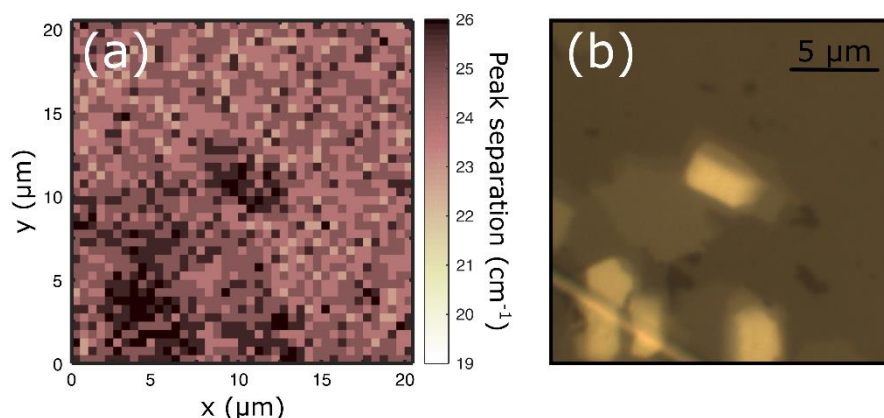


Figure S1: a) Raman map showing the difference between the E_{12g} and A_{1g} peaks. The map shows a large region of ~4 layers, according to the peak difference value, and a thicker region in the bottom left corner. b) Optical image of the same region studied in (a).

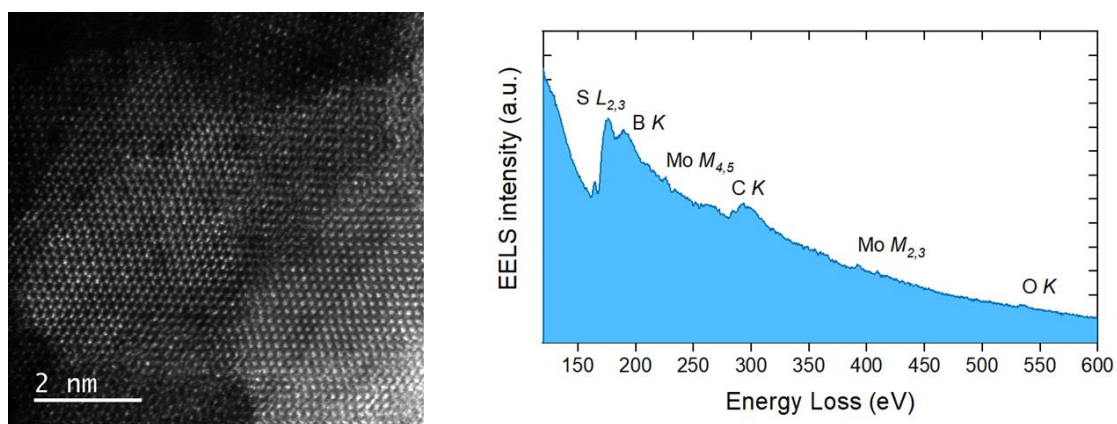


Figure S2: a) High magnification HAADF image of a MoS₂ thin film transferred over a holey Si₃N₄ membrane support. b) Electron energy loss spectra (EELS) acquired while scanning over the area in (a) for a total time of 20s.